

Enhanced Charge Order in a Photoexcited One-Dimensional Strongly Correlated System

Hantao Lu,¹ Shigetoshi Sota,² Hiroaki Matsueda,³ Janez Bonča,^{4,5} and Takami Tohyama¹

¹*Yukawa Institute for Theoretical Physics, Kyoto University, Kyoto, 606-8502, Japan*

²*Computational Materials Science Research Team, RIKEN AICS, Kobe, Hyogo 650-0047, Japan*

³*Sendai National College of Technology, Sendai, 989-3128, Japan*

⁴*Faculty of Mathematics and Physics, University of Ljubljana, SI-1000 Ljubljana, Slovenia*

⁵*J. Stefan Institute, SI-1000 Ljubljana, Slovenia*

(Dated: October 22, 2018)

We present a compelling response of a low-dimensional strongly correlated system to an external perturbation. Using the time-dependent Lanczos method we investigate a nonequilibrium evolution of the half-filled one-dimensional extended Hubbard model, driven by a transient laser pulse. When the system is close to the phase boundary, by tuning the laser frequency and strength, a sustainable charge order enhancement is found that is absent in the Mott insulating phase. We analyze the conditions and investigate possible mechanisms of emerging charge order enhancement. Feasible experimental realizations are proposed.

PACS numbers: 71.10.Fd, 74.40.Gh, 78.47.J-, 78.20.Bh

Nonequilibrium processes in strongly correlated electron systems can provide new insights into the dynamical properties of these systems, which, in many aspects, can be qualitatively different from their weakly interacting counterparts. One such example is nonequilibrium induced phase transition [1–3]. As the system is driven away from the equilibrium, under certain conditions, a “crossover” from one state to another (metastable) state may occur.

A well-known example is the insulator-to-metal transition induced either by strong electric field or transient laser pulse, as a result of photodoping [4–8]. In the case of Mott insulators, photocarriers are doublons and holons. In one dimension, just after the doping, generally, the system is in a metallic state due to the existence of itinerant carriers and the benefit of the spin-charge separation [8, 9]. Experimentally, the dielectric breakdown in one-dimensional (1D) Mott insulators has been observed long ago in organic materials [10, 11] and oxides [12]. Photoinduced metallic state by transient light has also been investigated [8, 13]. More recently, the nonequilibrium and nonlinear phenomena have stimulated significant interest within the cold atom community, where a novel realization of the fermionic Mott insulating state has been achieved [14].

In this Letter we address the question of whether it is possible to reach other characteristically different states besides the metallic one after the photodoping. One possibility is the enhancement of charge-order when the attractive interaction between doublons and holons is incorporated [15]. We seek such enhancement in the extended half-filled 1D Hubbard model with an additional nearest-neighbor interaction. At half filling, its phase is well-known and understood [16–19]. In large on-site Coulomb interaction, the model possesses two phases: spin-density-wave (SDW) and charge-density-wave (CDW), connected by a first order quantum phase transition, with algebraic decay of spin correlations and

long-range charge order, respectively. In general, as a correlated system approaches the phase boundary, the response to an external perturbation becomes more elaborate. In this Letter we show that in the latter case a substantial change in the electronic structure can be triggered by the optical pulse. In particular, when the system is originally in the Mott-insulating phase but close to the transition to CDW, a sustainable enhancement of charge order parameter is achieved by exposing the system to an external optical pulse with a rather carefully tuned frequency and amplitude.

We consider the 1D extended Hubbard model at half filling. The laser pump is incorporated by means of the Peierls substitution in the Hamiltonian:

$$\begin{aligned}
 H(t) = & -t_h \sum_{i,\sigma} \left(e^{iA(t)} c_{i,\sigma}^\dagger c_{i+1,\sigma} + \text{H.c.} \right) \\
 & + U \sum_i \left(n_{i,\uparrow} - \frac{1}{2} \right) \left(n_{i,\downarrow} - \frac{1}{2} \right) \\
 & + V \sum_i (n_i - 1) (n_{i+1} - 1), \quad (1)
 \end{aligned}$$

where $c_{i,\sigma}^\dagger$ ($c_{i,\sigma}$) creates (annihilates) electrons with spin σ at site i , $n_{i,\sigma} = c_{i,\sigma}^\dagger c_{i,\sigma}$, $n_i = n_{i,\uparrow} + n_{i,\downarrow}$, t_h is the hopping constant while U and V are the on-site and nearest neighbor interaction strengths, respectively. We model the external laser pulse in the temporal gauge via the time-dependent vector potential $A(t)$ [20]

$$A(t) = A_0 e^{-(t-t_0)^2/2t_d^2} \cos[\omega_{\text{pump}}(t-t_0)], \quad (2)$$

where A_0 controls the laser amplitude, which reaches its full strength at $t = t_0$; t_d characterizes the duration time of light action. Notice that due to finite t_d , the incoming photon frequency is broadened into a Gaussian-like distribution, with the variance of $1/t_d^2$ around the central value ω_{pump} . We set t_h and t_h^{-1} as energy and time units.

We now give a short overview of the equilibrium properties (with $A = 0$) of the model, related to our work. We set $U = 10$ and vary V . With increasing V the system undergoes around $U \approx 2V$ a first-order phase transition directly between SDW and CDW phases. Choosing rather large U we avoid the intermediate bond-order-wave phase that separates SDW and CDW at smaller U [17–19]. In both phases charge excitations are gapped. In the Mott insulating, i.e., SDW phase, gapless spin excitations exist and the system displays no charge order. In contrast, a charge-density wave is characteristic for the CDW phase while spin excitations are gapped.

In order to solve the time-dependent Hamiltonian $H(t)$, starting from the Schrödinger equation $i\partial\psi(t)/\partial t = H(t)\psi(t)$, we employ the time-dependent Lanczos method, which is originally described in Ref. [21] and later applied and analyzed in more detail in Ref. [22], followed by its applications in nonequilibrium dynamics of strongly correlated systems in Ref. [23]. The basic idea is that we approximate the time evolution of $|\psi(t)\rangle$ by a step-wise change of time t in small increments δt . At each step, the Lanczos basis with dimension M is generated resulting in the time evolution

$$|\psi(t + \delta t)\rangle \simeq e^{-iH(t)\delta t}|\psi(t)\rangle \simeq \sum_{l=1}^M e^{-i\epsilon_l\delta t}|\phi_l\rangle\langle\phi_l|\psi(t)\rangle, \quad (3)$$

where ϵ_l and $|\phi_l\rangle$, respectively, are eigenvalues and eigenvectors of the tridiagonal matrix generated in Lanczos iteration. We have confirmed that in our calculation, generally $M = 30$ provides adequate accuracy when $\delta t \lesssim 0.1$. For even smaller δt , M can be smaller.

In the succeeding numerical calculations, we employ periodic boundary conditions and set $t_d = 5$ and $t_0 = 12.5$. To investigate the time evolution of the charge order, we define the charge-charge correlation as

$$C(j; t) = \frac{(-1)^j}{L} \sum_{i=0}^{L-1} \langle \psi(t) | (n_{i+j} - 1)(n_i - 1) | \psi(t) \rangle, \quad (4)$$

where L is the lattice size.

Figure 1 shows the results of charge-charge correlation functions $C(j; t)$ for the system with 14 lattice sites, where the largest distance between two sites is 7. In order that the photon energy can be effectively transmitted to the electrons, we match the pumping frequency ω_{pump} with the first optical absorption peak. Figure 1(a) to 1(c) show the results of the system approaching the phase boundary from the SDW side, as the nearest-neighbor interaction V increases from 1.0 to 4.5 (while keeping fixed $U = 10$). For $V = 1.0$ and 3.0 the response of the system shows only a slight increase of mostly short-distance correlations during and after the pulse. In contrast, at $V = 4.5$ the system displays clear tendency towards a sustainable charge order enhancement that emerges as the external pulse reaches its maximum and remains nearly constant after the pulse. By performing a time-dependent density-matrix renormalization group

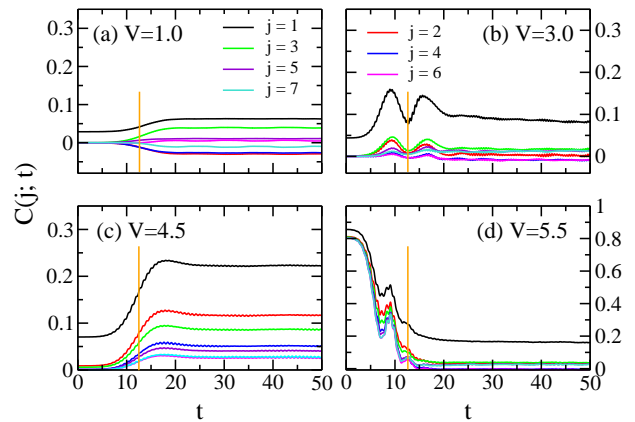


FIG. 1: (color online) Time dependence of the charge-charge correlations as functions of distance (labeled by j) for 14-site lattice. The laser pulse with Gaussian magnitude modulation reaches its full strength at $t = 12.5$, as indicated by solid lines. Without exception, the pumping frequencies are set to match the resonance peaks of the optical absorption spectrum. Parameters: $U = 10$, $\delta t = 0.02$, $M = 100$. (a) $V = 1.0$, $\omega_{\text{pump}} = 7.1$, $A_0 = 0.10$; (b) $V = 3.0$, $\omega_{\text{pump}} = 6.1$, $A_0 = 0.30$; (c) $V = 4.5$, $\omega_{\text{pump}} = 4.0$, $A_0 = 0.07$; (d) $V = 5.5$, $\omega_{\text{pump}} = 4.1$, $A_0 = 0.60$.

method under open boundary conditions on larger system size, up to 30, similar behavior can be observed (not shown here). We note that the length scale with which prominent charge order enhancement can be identified in the case of $V = 4.5$ is confined within distance less than ten, in the units of lattice constant. The opposite effect is found when starting from the CDW side of the phase diagram, at $V = 5.5$ [Fig. 1(d)], where after the pulse, the charge order is substantially diminished, along with a limited recovery of SDW order.

For deeper understanding of the photoinduced charge order enhancement we note that the quantum phase transition between SDW-CDW phases is driven by the competition between the energy cost for doublon generation and the energy gain due to the attraction between doublon-holon pairs. The transition point is roughly $V \approx U/2$. In the SDW phase, we expect charge-order favorite states to proliferate in the low energy regime as the transition point is approached, which makes them likely candidates to be picked up by the laser pulse. This is in contrast to the case when the system is far from the transition point where CDW states represent high-energy states. For a more quantitative analysis, we compare the spectra of systems with different values of V in the time-independent Hamiltonian, i.e., Eq. (1) but $A(t) = 0$. In order to describe the CDW order with finite spatial extension, we define

$$\mathcal{O}_{\text{CDW}} = \frac{1}{LL_c} \sum_{i=0}^{L-1} \sum_{j=1}^{L_c} (-1)^j (n_{i+j} - 1)(n_i - 1). \quad (5)$$

Here, L_c is introduced as a cut off parameter for the correlation length. The expectation values of the order

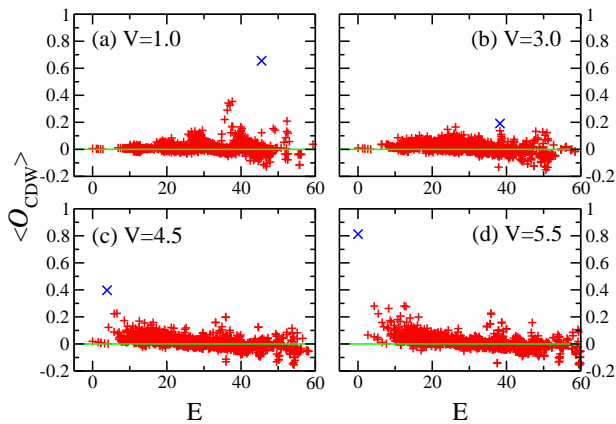


FIG. 2: (color online) The expectations of CDW order parameter of eigenstates for 10-site lattice with $V = 1.0, 3.0, 4.5,$ and 5.5 . The energy E is measured from the ground state. Only the data of states with $P_{\text{tot}} = S_{\text{tot}} = 0$ are shown, up to $E = 60$. Note that the largest value of $\langle \mathcal{O}_{\text{CDW}} \rangle$ in (a) through (d) is marked by a cross.

parameter $\langle \mathcal{O}_{\text{CDW}} \rangle$ for eigenstates of a smaller 10-site system with $L_c = 5$ are produced in Fig. 2. Comparison between different excited states shows that we can distinguish states with large values of the CDW order. Note that despite the external laser pulse, the total momentum P_{tot} and the total spin S_{tot} remain good quantum values throughout the time evolution. For the ground state of a 10-site lattice at half filling, we have $P_{\text{tot}} = S_{\text{tot}} = 0$. Accordingly, only results of the eigenstates with the same values of P_{tot} and S_{tot} are displayed.

In Fig. 2, we find that in the case of small $V = 1.0$, the eigenstates with predominant CDW features are positioned in the high energy regime, located around $E \sim 45$ above the ground state energy. With the increase of V the states with large values of $\langle \mathcal{O}_{\text{CDW}} \rangle$ move towards the lower part of the energy spectra. At $V = 5.5$ the eigenstate with $\langle \mathcal{O}_{\text{CDW}} \rangle \approx 0.65$ turns to be the ground state [Fig. 2(d)]. Keeping this picture in mind, it becomes more plausible that a well-tuned laser pulse may trigger the enhancement of the charge order on the SDW side of the phase diagram. Our numerical calculations suggest that the necessary precondition for such enhancement is the proximity of the system to the phase boundary as well as matching conserved quantum numbers between the SDW and CDW phases.

We further elaborate on the condition for the emergence of the CDW order enhancement induced by the laser pulse. To this effect we perform parameter-sweeping calculations on the 10-site lattice. We sweep the pumping frequency ω_{pump} and laser intensity A_0 and carry out the time evolutions up to $t = 52.5$. For a given pair of ω_{pump} and A_0 , we then calculate the expectation of CDW order $\langle \mathcal{O}_{\text{CDW}} \rangle_{\text{av}}$, and the energy increase measured from the ground state ΔE , by averaging on the last 50 time steps (corresponding to time length $\Delta t = 5$). Contour plots of $\langle \mathcal{O}_{\text{CDW}} \rangle_{\text{av}}$ and ΔE are shown in Fig. 3. To facil-

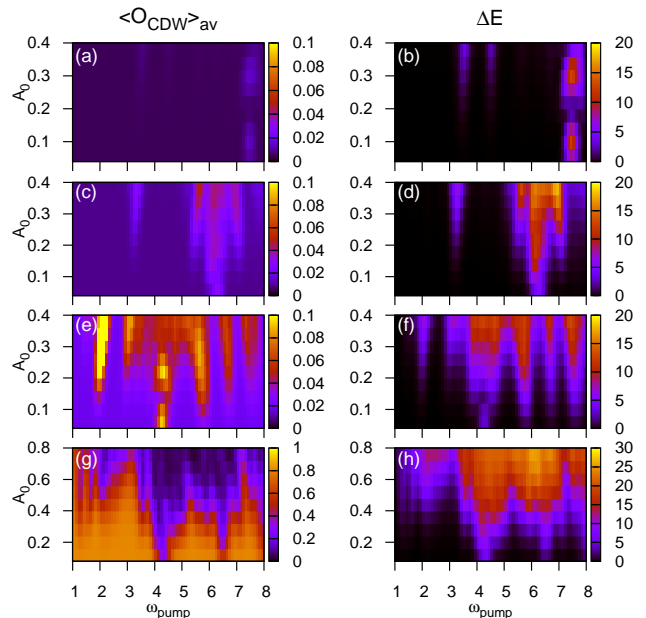


FIG. 3: (color online) Contour plots of final time-evolution results of CDW order $\langle \mathcal{O}_{\text{CDW}} \rangle_{\text{av}}$ (first column) and energy increase ΔE (second column) as functions of ω_{pump} and A_0 , obtained by averaging on the last 50 time steps (time length $\Delta t = 5$), for 10-site lattice. Here, we take $\delta t = 0.1$, $M = 30$. (a), (b) $V = 1.0$; (c), (d) $V = 3.0$; (e), (f) $V = 4.5$; and (g), (h) $V = 5.5$.

itate the analysis we present in Fig. 4 the corresponding optical spectra, obtained from the imaginary part of the dynamical current-current correlation function:

$$\text{Im}\chi_j(\omega) = \frac{1}{L} \sum_n \left| \langle n | \hat{j} | 0 \rangle \right|^2 \delta(\omega - E_n + E_0), \quad (6)$$

where $|0\rangle$ and $|n\rangle$ represent the ground state and excited states with energy E_0 and E_n , respectively. The current operator \hat{j} defined as $\hat{j} = -i \sum_{i,\sigma} (c_{i,\sigma}^\dagger c_{i+1,\sigma} - \text{H.c.})$.

In Fig. 3, we notice the emergence of similar patterns between $\langle \mathcal{O}_{\text{CDW}} \rangle_{\text{av}}$ (left) and ΔE (right) in each row panel. When starting from the SDW side [Figs. 3(a)-3(f)], in the case of moderate values of A_0 , the contour plots representing the CDW enhancement and energy increase roughly match. On the other hand, starting from the CDW ground state, when $V = 5.5$ [Figs. 3(g) and 3(h)], the effect is just the opposite: the energy increase occurs along the destruction of charge order. Furthermore, the positions of the enhanced energy stripes largely coincide with the resonance-peak positions of optical absorption, as presented in Fig. 4, except for some cases in the large A_0 region, which will be discussed later. From these observations, we can conclude that at moderate values of A_0 , in order to obtain enhanced $\langle \mathcal{O}_{\text{CDW}} \rangle_{\text{av}}$, the incoming photon frequency should be tuned close to absorption windows, that match resonance peaks of the optical spectrum.

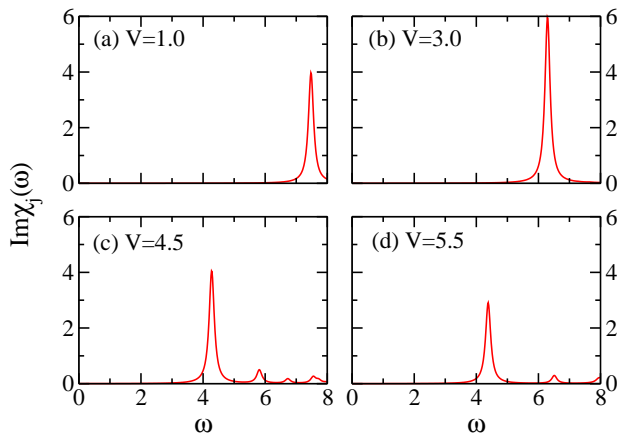


FIG. 4: (color online) The imaginary part of the dynamical current-current correlation function for 10-site lattice with $V = 1.0, 3.0, 4.5,$ and 5.5 , obtained by Lanczos method. The δ function is approached by a Lorentzian with a width of 0.1 .

Let us investigate the case of $V = 4.5$ in more detail. The first optical peak is located at $\omega \simeq 4.3$ [Fig. 4(c)]. States with enhanced CDW order are located around the same energy (the highest one with energy 3.9), as shown in Fig. 2(c). Not surprisingly, a sustainable enhancement of $\langle \mathcal{O}_{\text{CDW}} \rangle_{\text{av}}$ can be found with $\omega_{\text{pump}} \simeq 4.3$ when $A_0 \sim 0.08$ [Fig. 3(e)]. On the other hand, systems with $V = 1.0,$ and 3.0 [Figs. 3(a) and 3(c)] display no, or at most a very slight, increase of $\langle \mathcal{O}_{\text{CDW}} \rangle_{\text{av}}$ around the resonance frequencies, which match the optical frequency peaks, i.e., $\omega \simeq 7.5$ and 6.3 , respectively [Figs. 4(a) and 4(b)]. We thus propose two conditions for the observation of the enhancement of $\langle \mathcal{O}_{\text{CDW}} \rangle_{\text{av}}$ after the pulse: 1) the current matrix element $\langle n | \hat{j} | 0 \rangle$ in Eq. (6) should be sizable and 2) $\langle n | \mathcal{O}_{\text{CDW}} | n \rangle$ should be large as well.

Further detailed analysis on the $V = 4.5$ case shows that at $\omega_{\text{pump}} \simeq 4.3$, with A_0 growing beyond 0.1 , ΔE temporally drops, reaches a local minimum and then keeps increasing [Fig. 3(f)]. The CDW signal up to $A_0 \sim 0.25$ follows the same trend and then decreases [Fig. 3(e)]. This suggests a third condition to obtain enhancement of $\langle \mathcal{O}_{\text{CDW}} \rangle_{\text{av}}$: the pulse should deliver the optimal energy increase which can be controlled either by A_0 , or another parameter t_d . In some simulations we have noticed a temporary increase of CDW order that lasts only up to the midpoint of the pulse action and then diminishes. The reason is that the system has passed the CDW enhancement region during the process – it has gained excessive energy. Such a case can be found in Fig. 1(b) ($V = 3.0, A_0 = 0.30$), where we observe that two successive enhancements of the CDW signal appear during the pulse and then die out. The fact that the double-peak structure also emerges in the corresponding energy profile is consistent with the above argument. Moreover, during the irradiation, photons can be absorbed or emitted at different stages following the time evolution.

We also notice the enhancements of the CDW signal with the accompanying energy increase when ω_{pump} is less than the resonance frequency, such as for $V = 4.5$, when $\omega_{\text{pump}} \approx 2$ [Fig. 3(e)]. We speculate that this effect is generated by the multiphoton, or more precisely, two-photon process, partly supported by the fact that it appears at large A_0 and the energy increase is close to 4 , the same as what happens when the ω_{pump} is around 4 . The analysis on this possible multiphoton process in the off-resonant regime is out of reach of the present Letter [24].

In conclusion, we address the issues of the thermodynamic limit and feasible experimental realizations of the proposed CDW enhancement. It is well known that for the 1D extended Hubbard model, excitonic bound states can be found at the edge of the optical spectrum when $V \geq 2t_h$ [25]. The existence of well-formed excitons is a preliminary condition of the enhancement of the CDW order parameter after a laser pumping. With further increase of V , we can expect that at the edge of the absorption spectrum, charge-order states multiply and gradually dominate. They can thus be captured by a laser pulse with well tuned frequency and strength, as proposed by our numerical simulations.

Although it is quite difficult to find a quasi-1D Mott insulator with proper U and V values that position the system near the phase boundary, there are other mechanisms which can take up the role of V . When additional on-site Holstein phonons are taken into account, it has been shown that the system can be driven from SDW to CDW phase by electron-phonon interactions [26, 27]. Representative materials near the phase boundary with substantial electron-phonon interaction can be found in tetracyanoquinodimethane (TCNQ) series [28]. Another way to approach the phase boundary can be chemical substitutions, as in halogen-bridged transition metal compounds [29]. Moreover, a transient phase transition from CDW to Mott or metallic phases has already been observed [30]. These might prove to be useful in the search of proper candidates to observe the proposed effect. As an alternative to electronic systems, CDW enhancement can possibly be realized in cold atoms [31].

Finally, we would like to emphasize that, while our work has concentrated on a particular CDW order enhancement induced by a laser pulse, the proposed mechanism may be effective in other cases when observing the response of correlated systems to an external perturbation near a phase boundary such as enhanced antiferromagnetic correlations, stripes, or possibly even superconducting fluctuations.

This work was also supported by the Strategic Programs for Innovative Research (SPIRE), the Computational Materials Science Initiative (CMSI), the global COE program "Next Generation Physics, Spun from Universality and Emergence" from MEXT, the Yukawa International Program for Quark-Hadron Sciences at YITP, Kyoto University, and SLO-Japan collaboration project from ARRS and JSPS. T.T. acknowledges sup-

port by the Grant-in-Aid for Scientific Research (Grant No. 22340097) from MEXT. J.B. acknowledges support by the P1-0044 of ARRS, and CINT user program, Los Alamos National Laboratory, NM USA. A part of numer-

ical calculations was performed in the supercomputing facilities in YITP and ACCMS, Kyoto University, and ISSP in the University of Tokyo.

-
- [1] K. Yonemitsu and K. Nasu, *Phys. Rep.* **465**, 1 (2008).
 [2] K. Iwano, *Phys. Rev. B* **70**, 241102 (2004).
 [3] K. Iwano, *Phys. Rev. Lett.* **102**, 106405 (2009).
 [4] T. Oka, R. Arita, and H. Aoki, *Phys. Rev. Lett.* **91**, 066406 (2003).
 [5] T. Oka and H. Aoki, *Phys. Rev. Lett.* **95**, 137601 (2005).
 [6] A. Takahashi, H. Itoh, and M. Aihara, *Phys. Rev. B* **77**, 205105 (2008).
 [7] M. Eckstein, T. Oka, and P. Werner, *Phys. Rev. Lett.* **105**, 146404 (2010).
 [8] H. Okamoto, H. Matsuzaki, T. Wakabayashi, Y. Takahashi, and T. Hasegawa, *Phys. Rev. Lett.* **98**, 037401 (2007).
 [9] K. A. Al-Hassanieh, F. A. Reboredo, A. E. Feiguin, I. González, and E. Dagotto, *Phys. Rev. Lett.* **100**, 166403 (2008).
 [10] Y. Tokura, H. Okamoto, T. Koda, T. Mitani, and G. Saito, *Phys. Rev. B* **38**, 2215 (1988).
 [11] F. Sawano, I. Terasaki, H. Mori, T. Mori, M. Watanabe, N. Ikeda, Y. Nogami, and Y. Noda, *Nature* **437**, 522 (2005).
 [12] Y. Taguchi, T. Matsumoto, and Y. Tokura, *Phys. Rev. B* **62**, 7015 (2000).
 [13] S. Iwai, M. Ono, A. Maeda, H. Matsuzaki, H. Kishida, H. Okamoto, and Y. Tokura, *Phys. Rev. Lett.* **91**, 057401 (2003).
 [14] R. Jördens, N. Strohmaier, K. Günter, H. Moritz, and T. Esslinger, *Nature* **455**, 204 (2008).
 [15] H. Gomi, A. Takahashi, T. Ueda, H. Itoh, and M. Aihara, *Phys. Rev. B* **71**, 045129 (2005).
 [16] P. van Dongen, *Phys. Rev. B* **49**, 7904 (1994).
 [17] M. Nakamura, *Phys. Rev. B* **61**, 16377 (2000).
 [18] M. Tsuchiizu and A. Furusaki, *Phys. Rev. Lett.* **88**, 056402 (2002).
 [19] S. Ejima and S. Nishimoto, *Phys. Rev. Lett.* **99**, 216403 (2007).
 [20] H. Matsueda, S. Sota, T. Tohyama, and S. Maekawa, *J. Phys. Soc. Jpn.* **81**, 013701 (2012).
 [21] T. J. Park and J. C. Light, *J. Chem. Phys.* **85**, 5870 (1986).
 [22] N. Mohankumar and S. M. Auerbach, *Comput. Phys. Commun.* **175**, 473 (2006).
 [23] P. Prelovšek and J. Bonča, *ArXiv e-prints* (2011), arXiv:1111.5931 [cond-mat.str-el] .
 [24] T. Oka, *Phys. Rev. B* **86**, 075148 (2012).
 [25] H. Matsueda, T. Tohyama, and S. Maekawa, *Phys. Rev. B* **70**, 033102 (2004).
 [26] S. Ejima and H. Fehske, *J. Phys.: Conf. Ser.* **200**, 012031 (2010).
 [27] M. Tezuka, R. Arita, and H. Aoki, *Phys. Rev. B* **76**, 155114 (2007).
 [28] M. Kumar, B. J. Topham, R. Yu, Q. B. D. Ha, and Z. G. Soos, *J. Chem. Phys.* **134**, 234304 (2011).
 [29] M. Yamashita, T. Manabe, T. Kawashima, H. Okamoto, and H. Kitagawa, *Coord. Chem. Rev.* **190-192**, 309 (1999).
 [30] K. Kimura, H. Matsuzaki, S. Takaishi, M. Yamashita, and H. Okamoto, *Phys. Rev. B* **79**, 075116 (2009).
 [31] M. Lewenstein, A. Sanpera, V. Ahufinger, B. Damski, A. Sen De, and U. Sen, *Adv. Phys.* **56**, 243 (2007).